

Supporting Information

Kraushar et al. 10.1073/pnas.1408305111

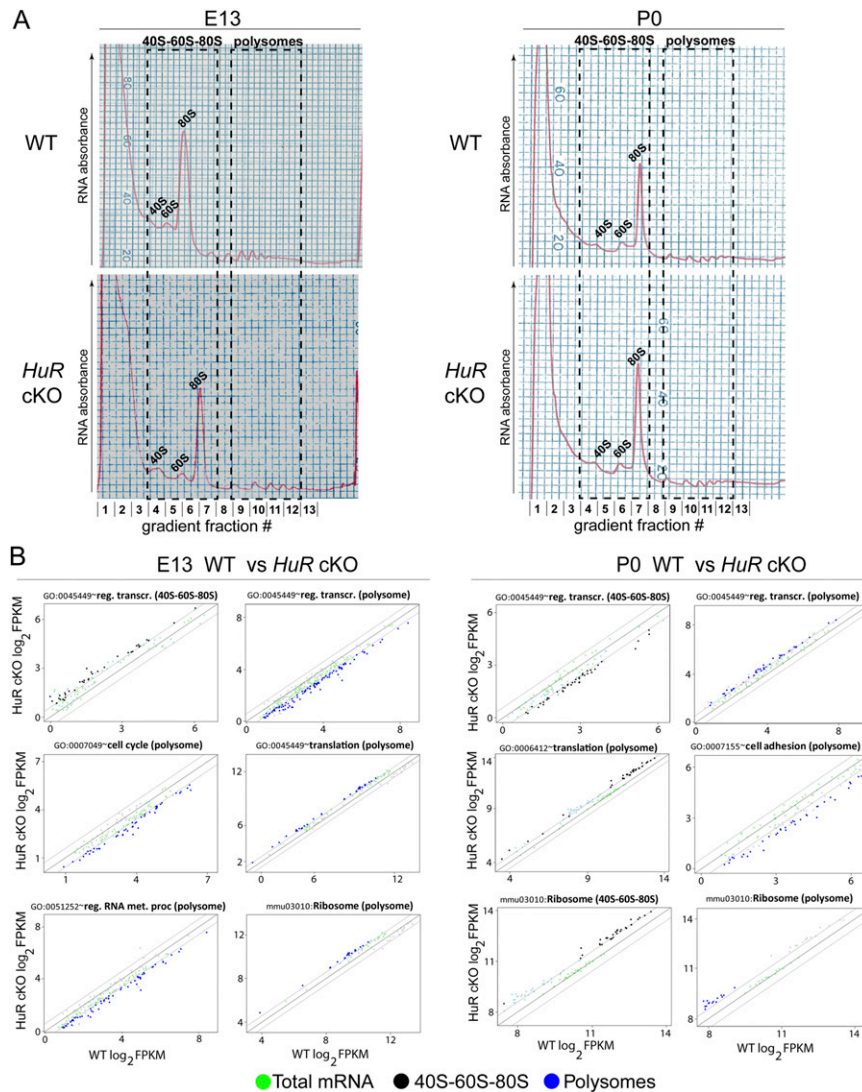


Fig. S1. Analysis of functionally related mRNAs regulated by Hu antigen R (HuR) in the neocortex at embryonic day 13 (E13) and postnatal day 0 (P0). (A) Representative curves of total RNA absorbance monitored during fractionation of WT and *HuR*-conditional knockout (*HuR*-cKO) neocortices at E13 and P0 ($n = 2$ cortices per fractionation). The 40S–60S–80S and polysome peaks are highlighted, corresponding to discrete fractions used for downstream analysis. (B) Plots show the relative mRNA expression levels of functionally related genes in WT and *Emx1*-*HuR*-cKO neocortices at E13 and P0, comparing total mRNAs, 40S–60S–80S-associated mRNAs, and polysome-associated mRNAs. Transcripts were measured with RNA sequencing (RNAseq) and analyzed by Kyoto Encyclopedia of Genes and Genomes (KEGG) and Gene Ontology (GO) bioinformatics (1, 2), with P values transformed to q values to control for false-discovery rates arising from multiple comparisons. Colored dots represent unique mRNAs within each functional group that differ between WT and *HuR*-cKO in total levels (green dots), in the 40S–60S–80S fraction (black dots), or in the polysomal fraction (blue dots). The mRNAs achieving statistical significance (surpassing a false-discovery rate of $\leq 5\%$; dotted lines) are highlighted, whereas those that are not statistically significant are clustered around the equivalence (solid line) region with a slope = 1. Fragments per kilobase of exon per million fragments mapped (FPKM) was calculated with TopHat and Cufflinks (3).

- Huang W, Sherman BT, Lempicki RA (2009) Bioinformatics enrichment tools: Paths toward the comprehensive functional analysis of large gene lists. *Nucleic Acids Res* 37(1):1–13.
- Huang W, Sherman BT, Lempicki RA (2009) Systematic and integrative analysis of large gene lists using DAVID bioinformatics resources. *Nat Protoc* 4(1):44–57.
- Trapnell C, et al. (2012) Differential gene and transcript expression analysis of RNA-seq experiments with TopHat and Cufflinks. *Nat Protoc* 7(3):562–578.

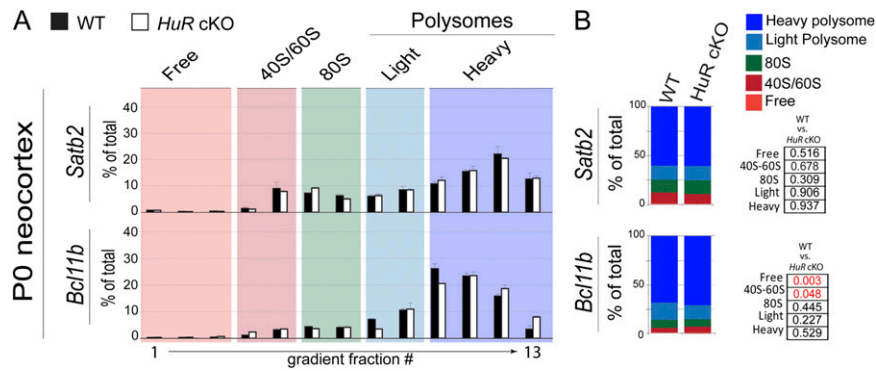


Fig. S2. HuR influences the polysomal positioning of distinct projection neuron mRNAs in the developing neocortex. (A) RNA was isolated from all 13 density-gradient fractions at P0, including the nontranslating free, 40S–60S, 80S, and the translating light and heavy polysomes. The mRNA candidate *Bcl11b* revealed by RNAseq was confirmed with quantitative RT-PCR (qRT-PCR) of WT (filled bars) and *HuR*-cKO (open bars), whereas *Satb2* was confirmed as an unchanged control. (B) Quantification and statistical analysis of the nontranslating and translating fractions are shown, comparing WT and *HuR*-cKO ($n = 4$ cortices in two fractionations; qRT-PCRs were performed in duplicate for each fraction). Statistical significance between WT and cKO for each category with t test is indicated in red text in *Right* ($P < 0.05$).

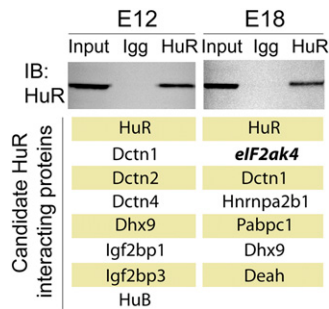


Fig. S3. Identification of HuR and eukaryotic initiation factor 2 alpha kinase 4 (*eIF2ak4*) interaction in the developing neocortex using coimmunoprecipitation. HuR immunoprecipitation from neocortical lysates at E12 and E18 was followed by mass spectrometry and target analysis. One of the most abundantly bound translation proteins was identified as *eIF2ak4*, which associates with HuR highly at E18 but less at E12. This increased association at E18 suggests a temporally dependent interaction with a translation control protein and was chosen as a target for investigating temporally defined control of neocortical polysome assembly.

A Translation candidates at P0 WT vs *HuR* cKO

	40S-60S-80S		Polysome	
	Protein ID	P	Protein ID	P
Initiation	Eif4A1	<0.01	Eif4A1	<0.01
	Eif4, gamma 1	<0.01	Eif2, sub. 3, X-linked	<0.01
	Eif2A	<0.01	Eif5A	<0.01
	Eif4A2	<0.01	Eif3, sub. B	<0.01
	Eif4, gamma 2	<0.01	Eif 4A2	<0.01
	Eif3, sub. A	<0.01	Eif3, sub. L	<0.01
	Eif 5A	0.01	Eif4, gamma 2	<0.01
	Eif2, sub. 3, X-linked	0.02	Eif3, sub.E	0.01
	Eif2, sub. 1 alpha	0.05	Eif 4, gamma 1	0.01
	Eif4H	0.05	Eif5	0.02
Elongation	EEF1 alpha 1	<0.01	Eef1 alpha 1	0.00
	EEF2	<0.01	Eef2	0.00
	EEF1 gamma	<0.01	Eef1 alpha 2	0.02
	EEF1 alpha 2	<0.01	Eef1 gamma	0.02
	EFTu GTP bind. dom.	0.04		
Ribosomal proteins	RPL10, pseud. 3	<0.01	RPS7	0.01
	RPL5	0.01	RPL5	0.01
	RPL3	0.01	RPL7A	0.01
	RPS12	0.01	RPLP0	0.02
	RPL13A	0.02	RPSA	0.02
	RPL9	0.03	RPS3	0.02
	RPL4	0.03	RPS15A	0.02
	RPL26	0.04	RPL8	0.03
	RPL37a	0.05	RPL10A	0.03
	RP L14	0.05	RPS27A	0.06
	RPL7	0.05	RPS4, X-linked	0.06
	RPS17	0.06		
	RPS13	0.06		
	RPS11	0.06		

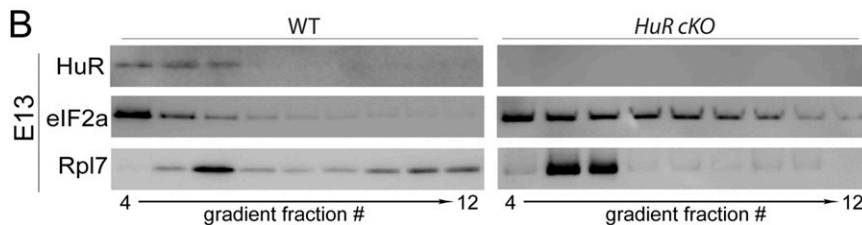


Fig. S4. Identification of *HuR*-regulated translation-associated proteins in 40S–60S–80S and polysomal fractions of developing neocortices. (A) Lysates from WT and *HuR*-cKO neocortices at E13 and P0 were fractionated by sucrose density-gradient ultracentrifugation, pooled into 40S–60S–80S and polysomal fractions, and analyzed by mass spectrometry coupled to bioinformatics. Proteins with significantly different abundances in these fractions were segregated into functionally related subgroups by KEGG analysis (shown for P0). The partitioning of many translation-associated proteins in 40S–60S–80S and polysomal fractions was disrupted by *HuR*-cKO, including initiation and elongation factors and ribosomal proteins. Several candidates were chosen for further investigation, including eIF5, eukaryotic elongation factor 1A1 (eEF1A1), ribosomal protein large 5 (Rpl5), and Rpl7; these were compared with eIF2a, which did not change in abundance in polysomal fractions. (B) Fractionated E13 neocortices ($n = 2$) were analyzed by Western blot to confirm that translation proteins were disrupted by *HuR* deletion in polysomes (Upper), such as Rpl7 (Lower), in the nascent neocortex.

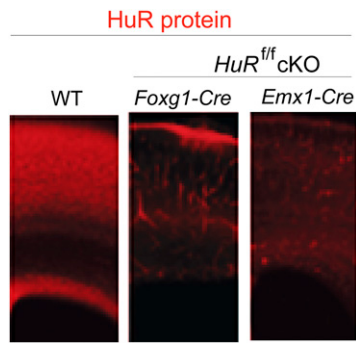


Fig. S5. Confirmation of HuR depletion in *HuR*-cKO neocortices. HuR immunohistochemical analysis (red) was performed on P0 neocortical coronal sections from WT, *Foxg1-HuR*-cKO, and *Emx1-HuR*-cKO. The results confirm that HuR protein is depleted in *HuR*-cKOs.

Primary antibodies

Name	Species	Cat. No.	Company	Concentration	Dilution
anti-Calbindin D28k	Rabbit	CB38	Swant		1:500 (immuno)
Bcl-11b (2586)	Rat	sc-56014	Santa Cruz Biotechnology	100 ug/ml	1:100 (immuno)
Cdp (M-222)	Rabbit	sc-13024	Santa Cruz Biotechnology	200 ug/ml	1:100 (immuno)
eEF1A1	Rabbit	ab157455	Abcam	1 mg/ml	1:250 (western)
eEF2	Rabbit	23325	Cell signaling	1 mg/ml	1:1000 (western)
eEF2 phospho (T56)	Rabbit	23315	Cell signaling	1 mg/ml	1:1000 (western)
eIF2a	Rabbit	53245	Cell signaling	1 mg/ml	1:1000 (western)
eIF2a phospho (551)	Rabbit	33985	Cell signaling	1 mg/ml	1:1000 (western)
eIF2ak4/GCN2	Rabbit	33025	Cell signaling	1 mg/ml	1:250 (immuno), 1:1000 (western)
eIF3a	Rabbit	25385	Cell signaling	1 mg/ml	1:250 (western)
eIF4G (H-300)	Rabbit	sc-11373	Santa Cruz Biotechnology	200 ug/ml	1:250 (western)
eIF5	Rabbit	ab170915	Abcam	1 mg/ml	1:250 (western)
GFAP	Rabbit	G9269	Sigma Aldrich	9.1 mg/ml	1:100 (immuno)
GAPDH	Mouse	MAB374	Millipore	1 mg/ml	1:5000 (western)
pHistone H3	Rabbit	06-570	Millipore	1 mg/ml	1:500 (immuno)
HuR (19F12)	Mouse	sc-56709	Santa Cruz Biotechnology	100 ug/ml	1:1000 (immuno), 1:500 (western)
HuR (N16)	Goat	sc-5483	Santa Cruz Biotechnology	200 ug/ml	1:1000 (immuno)
L1	Rat	MAB5272	Millipore	1 mg/ml	1:500 (immuno)
Map2	Mouse	M9942	Sigma Aldrich	2 mg/ml	1:500 (immuno)
Pabp	Rabbit	49925	Cell signaling	1 mg/ml	1:100 (western)
Pax-6	Rabbit	PRB-278P	Covance	2 mg/ml	1:100 (immuno)
Rpl5	Rabbit	ab157099	Abcam	1 mg/ml	1:250 (western)
Rpl7	Rabbit	ab72550	Abcam	0.2 mg/ml	1:1000 (western)
Satb2	Mouse	ab51502	Abcam	0.1 mg/ml	1:100 (immuno)
Tbr2	Rabbit	ab23345	Abcam	1 mg/ml	1:500 (immuno)
Tle4 (E10)	Mouse	sc-365406	Santa Cruz Biotechnology	200 ug/ml	1:200 (immuno)

qRT-PCR probes

Probe	TaqMan Cat. No.
SATB2	Mm00507337_m1
BCL11B	Mm00480516_m1
CDH1	Mm01247357_m1
RPLP0	Mm00725448_s1
RPS27	Mm01218196_g1
RPS26	Mm02601831_g1

Fig. S6. Antibodies (*Upper*) and qRT-PCR probes (*Lower*).